

# Neutrinoless $\beta\beta$ decay transition matrix elements within mechanisms involving light Majorana neutrinos, classical Majorons, and sterile neutrinos

P. K. Rath,<sup>1</sup> R. Chandra,<sup>2,\*</sup> K. Chaturvedi,<sup>3</sup> P. Lohani,<sup>1</sup> P. K. Raina,<sup>4</sup> and J. G. Hirsch<sup>5</sup>

<sup>1</sup>Department of Physics, University of Lucknow, Lucknow-226007, India

<sup>2</sup>Department of Applied Physics, Babasaheb Bhimrao Ambedkar University, Lucknow-226025, India

<sup>3</sup>Department of Physics, Bundelkhand University, Jhansi-284128, India

<sup>4</sup>Department of Physics, Indian Institute of Technology, Ropar, Rupnagar-140001, India

<sup>5</sup>Instituto de Ciencias Nucleares, Universidad Nacional Autónoma de México, 04510 México, D.F., México

(Received 2 August 2013; revised manuscript received 7 November 2013; published 20 December 2013)

In the projected-Hartree-Fock-Bogoliubov (PHFB) model, uncertainties in the nuclear transition matrix elements for the neutrinoless double- $\beta$  decay of  $^{94,96}\text{Zr}$ ,  $^{98,100}\text{Mo}$ ,  $^{104}\text{Ru}$ ,  $^{110}\text{Pd}$ ,  $^{128,130}\text{Te}$ , and  $^{150}\text{Nd}$  isotopes within mechanisms involving light Majorana neutrinos, classical Majorons, and sterile neutrinos are statistically estimated by considering sets of 16 (24) matrix elements calculated with four different parametrizations of the pairing plus multipolar type of effective two-body interaction, two sets of form factors, and two (three) different parametrizations of Jastrow type of short-range correlations. In the mechanisms involving the light Majorana neutrinos and classical Majorons, the maximum uncertainty is about 15% and in the scenario of sterile neutrinos, it varies in between approximately 4 (9)%–20 (36)% without(with) Jastrow short range correlations with the Miller-Spencer parametrization, depending on the considered mass of the sterile neutrinos.

DOI: 10.1103/PhysRevC.88.064322

PACS number(s): 21.60.Jz, 23.20.-g, 23.40.Hc

## I. INTRODUCTION

In the last decade, the confirmation of neutrino flavor oscillations at atmospheric, solar, reactor, and accelerator neutrino sources [1,2] and the reported observation of neutrinoless double beta ( $\beta\beta$ )<sub>0ν</sub> decay [3–8] have together played an extremely inspirational role in the advancement of a vast amount of experimental as well as theoretical studies on nuclear double- $\beta$  decay in general and ( $\beta\beta$ )<sub>0ν</sub> decay in particular [9,10]. The former has provided information on the neutrino mass square differences  $\Delta m_{21}^2$  and  $\Delta m_{31}^2$ , mixing angles  $\theta_{12}$ ,  $\theta_{23}$ , and  $\theta_{13}$  and possible hierarchies in the neutrino mass spectrum [11]. In addition to hinting on the Majorana nature of neutrinos, the latter has also ascertained the role of various mechanism in different gauge theoretical models [12]. Presently, a number of projects for observing the ( $\beta\beta$ )<sub>0ν</sub> decay of  $^{48}\text{Ca}$  (CANDLES),  $^{76}\text{Ge}$  (GERDA, MAJORANA),  $^{82}\text{Se}$  (SuperNEMO, Lucifer),  $^{100}\text{Mo}$  (MOON, Amore),  $^{116}\text{Cd}$  (COBRA),  $^{130}\text{Te}$  (CUORE),  $^{136}\text{Xe}$  (XMASS, EXO, KamLand-Zen, NEXT),  $^{150}\text{Nd}$  (SNO ++, SuperNEMO, DCBA/MTD) [13–15] have been designed and hopefully, the reported observation of ( $\beta\beta$ )<sub>0ν</sub> decay [3,4] would be confirmed in the near future.

In the left-right symmetric model [16,17], the three possible mechanisms of ( $\beta^- \beta^-$ )<sub>0ν</sub> decay are the exchange of left handed light as well as heavy Majorana neutrinos and the exchange of right handed heavy Majorana neutrinos. Alternatively, the occurrence of lepton number violating Majoron accompanied ( $\beta\beta$ )<sub>0ν</sub> decay is also a possibility. Based on the most recent experimental evidences [18–21], regarding the observability of all nine Majoron models [22,23], it has been concluded that the study of classical Majoron models is the most preferred one.

In the short base line experiments [24,25], the indication of  $\bar{\nu}_\mu \rightarrow \bar{\nu}_e$  conversion was explained with  $0.2 \text{ eV} < \Delta m^2 < 2 \text{ eV}$  and  $10^{-3} < \sin^2 2\theta < 4 \cdot 10^{-2}$ . New results of the reactor fluxes favor short base line oscillation [26–28]. The confirmation of all these observations would imply the existence of more than three massive neutrinos [29]. In Ref. [22], it was shown that the mixing of a light sterile neutrino (mass  $\ll 1 \text{ eV}$ ) with a much heavier sterile neutrino (mass  $\gg 1 \text{ GeV}$ ) would result in observable signals in current  $\beta\beta$  decay experiments, as is the case in other interesting alternative scenarios [30,31].

The study of ( $\beta^- \beta^-$ )<sub>0ν</sub> decay within mechanisms involving light Majorana neutrinos, classical Majorons and sterile neutrinos can be performed under a common theoretical formalism [32–34]. In the mass mechanism, the contributions of the pseudoscalar and weak magnetism terms of the recoil current can change the nuclear transition matrix elements (NTMEs)  $M^{(0\nu)}$  up to 30% in the QRPA [35,36], about 20% in the interacting shell model (ISM) [37] and 15% in the interacting boson model (IBM) [38].

In the evaluation of NTMEs, the most desirable approach is to employ the successful large scale shell-model calculations [37,39–41], if feasible. However, the quasiparticle random phase approximation (QRPA) [42,43] and its extensions [44,45] have emerged as the most employed models for explaining the observed suppression of  $M_{2\nu}$  in addition to correlating the single- $\beta$  GT strengths and half-lives of ( $\beta^- \beta^-$ )<sub>2ν</sub> decay by including a large number of basis states in the model space. The necessity for the inclusion of nuclear deformation has resulted in the employment of deformed QRPA [46–48], projected-Hartree-Fock-Bogoliubov (PHFB) [49–52], pseudo-SU(3) [53], IBM [38,54–56], and energy density functional (EDF) [57] approaches in the calculation of NTMEs. Additionally, there are many possibilities for the inclusion of the model dependent form factors for the finite size of nucleons (FNS), short-range correlations (SRC) [53,58–62], and the value of axial vector current coupling constant  $g_A$ .

\*Corresponding author: ramesh\_dap@bbau.ac.in

[63]. Each model has a different truncation scheme for the unmanageable Hilbert space, and employs a variety of residual interactions, resulting in NTMEs  $M^{(0\nu)}$ , which are of the same order of magnitude but not identical.

In the analysis of uncertainties in NTMEs for  $(\beta^- \beta^-)_{0\nu}$  decay, the spread between the available calculated results [64] was translated into an average of all the available NTMEs, and the standard deviation was treated as the measure of the theoretical uncertainty [65,66]. Bilensky and Grifols [67] have suggested that the possible observation of  $(\beta\beta)_{0\nu}$  decay in several nuclei could be employed to check the calculated NTMEs in a model independent way by comparing the ratios of the NTMEs-squared with the ratios of observed half-lives  $T_{1/2}^{0\nu}$ . Model specific theoretical uncertainties have been analyzed in the QRPA approach [68–70]. Further, studies on uncertainties in NTMEs due to the SRC have also been preformed in Refs. [60,62,71].

The main objective of the present work is to study the effects of pseudoscalar and weak magnetism terms on the Fermi, Gamow-Teller (GT), and tensorial NTMEs for the  $(\beta^- \beta^-)_{0\nu}$  decay of  $^{94,96}\text{Zr}$ ,  $^{98,100}\text{Mo}$ ,  $^{104}\text{Ru}$ ,  $^{110}\text{Pd}$ ,  $^{128,130}\text{Te}$ , and  $^{150}\text{Nd}$  isotopes in the light Majorana neutrino mass mechanism. In addition, we investigate effects due to deformation, FNS, and the SRC vis-a-vis the radial evolution of NTMEs. Uncertainties in NTMEs are calculated statistically by employing four different parametrizations of effective two-body interaction, form factors with two different parametrizations, and three different parametrizations of the SRC. In the same theoretical formalism, the  $(\beta^- \beta^-)_{0\nu}$  decay involving classical Majorons and sterile neutrinos is also studied. The theoretical formalisms to calculate the half-lives of the  $(\beta^- \beta^-)_{0\nu}$  decay with induced currents [35,36], classical Majorons [33,35], and sterile neutrinos [31] have already been reported. Hence, we briefly outline the steps of the above derivations in Sec. II. In Sec. III, we present the results and discuss them vis-a-vis the existing calculations done in other nuclear models. Finally, the conclusions are given in Sec. IV.

## II. THEORETICAL FRAMEWORK

The detailed theoretical formalism required for the study of  $(\beta^- \beta^-)_{0\nu}$  decay due to the exchange of light Majorana neutrinos has been given by Šimkovic *et al.* [35] as well as Vergados [36]. The observability of Majoron accompanied  $(\beta^- \beta^-)_{0\nu}$  decay in nine Majoron models [22] has already been discussed by Hirsch *et al.* [23]. Further, the  $(\beta^- \beta^-)_{0\nu}$  decay within the mechanism involving sterile neutrinos has been given by Benes *et al.* [31]. In the following, we present a brief outline of the required theoretical formalism for the clarity in notations used in the present paper.

### A. Light Majoron neutrino mass mechanism

In the Majorana neutrino mass mechanism, the half-life  $T_{1/2}^{(0\nu)}$  for the  $0^+ \rightarrow 0^+$  transition of  $(\beta^- \beta^-)_{0\nu}$  decay due to the exchange of light Majorana neutrinos between nucleons having finite size is given by [35,36]

$$[T_{1/2}^{(0\nu)}(0^+ \rightarrow 0^+)]^{-1} = G_{01} \left| \frac{\langle m_\nu \rangle}{m_e} M^{(0\nu)} \right|^2, \quad (1)$$

where

$$\langle m_\nu \rangle = \sum_i' U_{ei}^2 m_i, \quad m_i < 10 \text{ eV}, \quad (2)$$

$$G_{01} = \left[ \frac{2(G_F g_A)^4 m_e^9}{64\pi^5 (m_e R)^2 \ln(2)} \right] \times \int_1^{T+1} F_0(Z_f, \varepsilon_1) F_0(Z_f, \varepsilon_2) p_1 p_2 \varepsilon_1 \varepsilon_2 d\varepsilon_1, \quad (3)$$

and in the closure approximation, the NTME  $M^{(0\nu)}$  is defined as

$$M^{(0\nu)} = \sum_{n,m} \langle 0_F^+ \parallel \left[ -\frac{H_F(r_{nm})}{g_A^2} + \sigma_n \cdot \sigma_m H_{\text{GT}}(r_{nm}) + S_{nm} H_T(r_{nm}) \right] \tau_n^+ \tau_m^+ \parallel 0_I^+ \rangle, \quad (4)$$

with

$$S_{nm} = 3(\sigma_n \cdot \hat{\mathbf{r}}_{nm})(\sigma_m \cdot \hat{\mathbf{r}}_{nm}) - \sigma_n \cdot \sigma_m. \quad (5)$$

The neutrino potentials associated with Fermi, Gamow-Teller (GT), and tensor operators are given by

$$H_\alpha(r_{nm}) = \frac{2R}{\pi} \int \frac{f_\alpha(qr_{nm})}{(q + \bar{A})} h_\alpha(q) q dq, \quad (6)$$

where  $f_\alpha(qr_{nm}) = j_0(qr_{nm})$  and  $f_\alpha(qr_{nm}) = j_2(qr_{nm})$  for  $\alpha = \text{Fermi/GT}$  and tensor potentials, respectively. The effects due to the FNS are incorporated through the dipole form factors and the form factor related functions  $h_F(q)$ ,  $h_{\text{GT}}(q)$  and  $h_T(q)$  are written as

$$h_F(q) = g_V^2(q^2), \quad (7)$$

$$h_{\text{GT}}(q) = \frac{g_A^2(q^2)}{g_A^2} \left[ 1 - \frac{2}{3} \frac{g_P(q^2)q^2}{g_A(q^2)2M_p} + \frac{1}{3} \frac{g_P^2(q^2)q^4}{g_A^2(q^2)4M_p^2} \right] + \frac{2}{3} \frac{g_M^2(q^2)q^2}{g_A^2 4M_p^2} \approx \left( \frac{\Lambda_A^2}{q^2 + \Lambda_A^2} \right)^4 \left[ 1 - \frac{2}{3} \frac{q^2}{(q^2 + m_\pi^2)} + \frac{1}{3} \frac{q^4}{(q^2 + m_\pi^2)^2} \right] + \left( \frac{g_V}{g_A} \right)^2 \frac{\kappa^2 q^2}{6M_p^2} \left( \frac{\Lambda_V^2}{q^2 + \Lambda_V^2} \right)^4, \quad (8)$$

$$h_T(q) = \frac{g_A^2(q^2)}{g_A^2} \left[ \frac{2}{3} \frac{g_P(q^2)q^2}{g_A(q^2)2M_p} - \frac{1}{3} \frac{g_P^2(q^2)q^4}{g_A^2(q^2)4M_p^2} \right] + \frac{1}{3} \frac{g_M^2(q^2)q^2}{g_A^2 4M_p^2} \approx \left( \frac{\Lambda_A^2}{q^2 + \Lambda_A^2} \right)^4 \left[ \frac{2}{3} \frac{q^2}{(q^2 + m_\pi^2)} - \frac{1}{3} \frac{q^4}{(q^2 + m_\pi^2)^2} \right] + \left( \frac{g_V}{g_A} \right)^2 \frac{\kappa^2 q^2}{12M_p^2} \left( \frac{\Lambda_V^2}{q^2 + \Lambda_V^2} \right)^4, \quad (9)$$

where

$$g_V(q^2) = g_V \left( \frac{\Lambda_V^2}{q^2 + \Lambda_V^2} \right)^2, \quad (10)$$

$$g_A(q^2) = g_A \left( \frac{\Lambda_A^2}{q^2 + \Lambda_A^2} \right)^2, \quad (11)$$

$$g_P(q^2) = \frac{2M_p g_A(q^2)}{(q^2 + m_\pi^2)} \left( \frac{\Lambda_A^2 - m_\pi^2}{\Lambda_A^2} \right), \quad (12)$$

$$g_M(q^2) = \kappa g_V(q^2) \quad (13)$$

with  $g_V = 1.0$ ,  $g_A = 1.254$ ,  $\kappa = \mu_p - \mu_n = 3.70$ ,  $\Lambda_V = 0.850$  GeV, and  $\Lambda_A = 1.086$  GeV. The presence of pseudoscalar and weak magnetism terms of the higher order currents (HOC) [35], results as seen by the consideration of Eqs. (4)–(13), in no change of the Fermi matrix element  $M_F^{(0\nu)} = -g_A^2 M_{F-VV}^{(0\nu)}$ , the addition of three new terms  $M_{GT-AP}^{(0\nu)}$ ,  $M_{GT-PP}^{(0\nu)}$ ,  $M_{GT-MM}^{(0\nu)}$  to the conventional GT  $M_{GT}^{(0\nu)} = M_{GT-AA}^{(0\nu)}$  matrix element and the addition of three new terms  $M_{T-AP}^{(0\nu)}$ ,  $M_{T-PP}^{(0\nu)}$ ,  $M_{T-MM}^{(0\nu)}$  as the tensor matrix element  $M_T^{(0\nu)}$ .

Consideration of internal structure of protons and neutrons suggests an alternative parametrization of  $g_V(q^2)$  given by [72]

$$g_V(q^2) = F_1^p(q^2) - F_1^n(q^2), \quad (14)$$

where

$$F_1^p(q^2) = \frac{1}{\left(1 + \frac{q^2}{4M^2}\right)} \left( \frac{\Lambda_V^2}{q^2 + \Lambda_V^2} \right)^2 \left[ 1 + (1 + \mu_p) \frac{q^2}{4M^2} \right], \quad (15)$$

$$F_1^n(q^2) = \frac{\mu_n}{\left(1 + \frac{q^2}{4M^2}\right)} \left( \frac{\Lambda_V^2}{q^2 + \Lambda_V^2} \right)^2 (1 - \xi_n) \frac{q^2}{4M^2} \quad (16)$$

with  $\mu_p = 1.79$  nm,  $\mu_n = -1.91$  nm, and  $\Lambda_V = 0.84$  GeV.

In addition,

$$g_M(q^2) = F_2^p(q^2) - F_2^n(q^2), \quad (17)$$

where

$$F_2^p(q^2) = \frac{\mu_p}{\left(1 + \frac{q^2}{4M^2}\right)} \left( \frac{\Lambda_V^2}{q^2 + \Lambda_V^2} \right)^2, \quad (18)$$

$$F_2^n(q^2) = \frac{\mu_n}{\left(1 + \frac{q^2}{4M^2}\right)} \left( \frac{\Lambda_V^2}{q^2 + \Lambda_V^2} \right)^2 \left( 1 + \frac{q^2}{4M^2} \xi_n \right) \quad (19)$$

with

$$\xi_n = \frac{1}{1 + \lambda_n \frac{q^2}{4M^2}} \quad (20)$$

and  $\lambda_n = 5.6$ . We get two sets of form factors by considering Eqs. (10)–(13) and Eqs. (11), (12), (14), (17), which are denoted by FNS1 and FNS2, respectively. In Fig. 1, we present the plot of  $g_V(q^2)$  and  $g_M(q^2)$  of FNS1 and FNS2, the shapes of which have definite relation with the magnitudes of NTMEs  $M^{(0\nu)}$ .

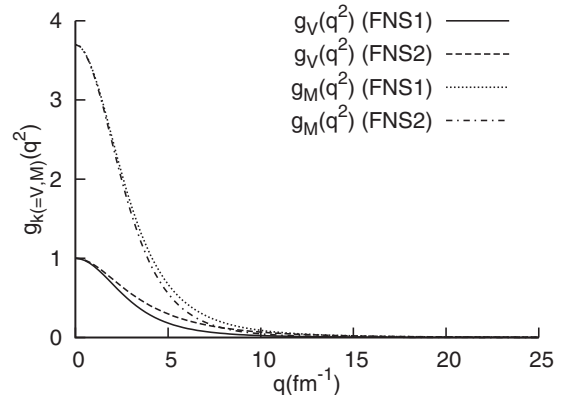


FIG. 1. Distribution of  $g_V(q^2)$  and  $g_M(q^2)$  for FNS1 and FNS2.

### B. Majoron accompanied $(\beta^- \beta^-)_{0\nu}$ decay

In the classical Majoron model, the inverse half-life  $T_{1/2}^{(0\nu\phi)}$  for the  $0^+ \rightarrow 0^+$  transition of Majoron emitting  $(\beta^- \beta^- \phi)_{0\nu}$  decay is given by [33,35]

$$[T_{1/2}^{(0\nu\phi)}(0^+ \rightarrow 0^+)]^{-1} = |\langle g_M \rangle|^2 G_{0M} |M^{(0\nu\phi)}|^2, \quad (21)$$

where  $\langle g_M \rangle$  is the effective Majoron-neutrino coupling constant and the NTME  $M^{(0\nu\phi)}$  is the same as the  $M^{(0\nu)}$  for the exchange of light Majorana neutrinos. The phase space factors  $G_{0M}$  are evaluated by using

$$G_{0M} = \left[ \frac{2(G_F g_A)^4 m_e^9}{256\pi^7 (m_e R)^2 \ln(2)} \right] \times \int_1^{T+1} F_0(Z_f, \varepsilon_1) p_1 \varepsilon_1 d\varepsilon_1 \times \int_1^{T+2-\varepsilon_1} (T+2-\varepsilon_1-\varepsilon_2) F_0(Z_f, \varepsilon_2) p_2 \varepsilon_2 d\varepsilon_2, \quad (22)$$

and have been calculated for all nuclei of general interest [23,73].

### C. Mechanism involving sterile neutrinos

The contribution of the sterile  $\nu_h$  neutrino to the half-life  $T_{1/2}^{(0\nu)}$  for the  $0^+ \rightarrow 0^+$  transition of  $(\beta^- \beta^-)_{0\nu}$  decay has been derived by considering the exchange of a Majorana neutrino between two nucleons and is given by [31]

$$[T_{1/2}^{(0\nu)}(0^+ \rightarrow 0^+)]^{-1} = G_{01} \left| U_{eh}^2 \frac{m_h}{m_e} M^{0\nu}(m_h) \right|^2, \quad (23)$$

where the phase space factor  $G_{01}$  is the same as Eq. (3),  $U_{eh}$  is the  $\nu_h - \nu_e$  mixing matrix element and the NTME  $M^{0\nu}(m_h)$  is written as

$$M^{0\nu}(m_h) = \langle 0_F^+ | \left[ -\frac{H_F(m_h, r)}{g_A^2} + \sigma_n \cdot \sigma_m H_{GT}(m_h, r) + S_{nm} H_T(m_h, r) \right] \tau_n^+ \tau_m^+ | 0_I^+ \rangle. \quad (24)$$

TABLE I. Decomposition of NTMEs  $M^{(0\nu)}$  for the  $(\beta^-\beta^-)_{0\nu}$  decay of  $^{100}\text{Mo}$  including higher order currents (HOC) with (a) FNS1, (b) FNS2 and SRC (HOC+SRC) for the  $PQQ1$  parametrization.

NTMEs	FNS	HOC	HOC + SRC			HOC + SRC ( $\bar{A}/2$ )		
			SRC1	SRC2	SRC3	SRC1	SRC2	SRC3
$M_F^{(0\nu)}$	(a)	2.1484	1.8911	2.1492	2.2216	2.0691	2.3412	2.4168
	(b)	2.2034	1.9152	2.1883	2.2707	2.0943	2.3817	2.4673
$M_{\text{GT-AA}}^{(0\nu)}$		-6.3815	-5.4584	-6.3022	-6.5663	-5.9813	-6.8682	-7.1424
$M_{\text{GT-PP}}^{(0\nu)}$		-0.4503	-0.2962	-0.4054	-0.4510	-0.3060	-0.4177	-0.4640
$M_{\text{GT-AP}}^{(0\nu)}$		1.5521	1.1518	1.4644	1.5810	1.2013	1.5222	1.6413
$M_{\text{GT-MM}}^{(0\nu)}$	(a)	-0.2370	-0.1192	-0.1832	-0.2201	-0.1239	-0.1892	-0.2266
	(b)	-0.2311	-0.1222	-0.1850	-0.2187	-0.1269	-0.1909	-0.2251
$M_{\text{GT}}^{(0\nu)}$	(a)	-5.5167	-4.7220	-5.4265	-5.6564	-5.2098	-5.9529	-6.1918
	(b)	-5.5107	-4.7250	-5.4283	-5.6549	-5.2128	-5.9546	-6.1902
$M_{T-\text{PP}}^{(0\nu)}$		-0.0227	-0.0230	-0.0235	-0.0234	-0.0236	-0.0241	-0.0240
$M_{T-\text{AP}}^{(0\nu)}$		0.0692	0.0700	0.0710	0.0709	0.0718	0.0729	0.0728
$M_{T-\text{MM}}^{(0\nu)}$	(a)	0.0059	0.0060	0.0062	0.0062	0.0061	0.0064	0.0064
	(b)	0.0058	0.0058	0.0060	0.0060	0.0059	0.0062	0.0062
$M_T^{(0\nu)}$	(a)	0.0524	0.0529	0.0538	0.0537	0.0543	0.0552	0.0551
	(b)	0.0522	0.0528	0.0536	0.0535	0.0542	0.0550	0.0549
$M^{(0\nu)}$	(a)	6.8305	5.8716	6.7394	7.0155	6.4712	7.3865	7.6736
	(b)	6.8597	5.8902	6.7664	7.0454	6.4904	7.4142	7.7044

In Eq. (24), the neutrino potentials are of the form

$$H_\alpha(m_h, r) = \frac{2R}{\pi} \int_0^\infty \frac{f_\alpha(qr) h_\alpha(q^2) q^2 dq}{\sqrt{q^2 + m_h^2} (\sqrt{q^2 + m_h^2} + \bar{A})}, \quad (25)$$

with the same  $h_\alpha(q^2)$  as given in Eqs. (7)–(9).

#### D. Uncertainties in NTMEs within PHFB model

In the PHFB model, the calculation of the NTMEs  $M_k^{(0\nu)}$  of the  $(\beta^-\beta^-)_{0\nu}$  decay has already been discussed in Ref. [50]. Employing the HFB wave functions, one obtains the following expression for the NTME  $M_k^{(0\nu)}$  of the  $(\beta^-\beta^-)_{0\nu}$  decay corresponding to an operator  $O_k$  [50]:

$$\begin{aligned} M_k^{(0\nu)} &= [n^{J_f=0} n^{J_i=0}]^{-1/2} \int_0^\pi n_{(Z,N),(Z+2,N-2)}(\theta) \sum_{\alpha\beta\gamma\delta} \langle \alpha\beta | O_k | \gamma\delta \rangle \\ &\times \sum_{\varepsilon\eta} \frac{(f_{Z+2,N-2}^{(\pi)*})_{\varepsilon\beta}}{[(1 + F_{Z,N}^{(\pi)}(\theta) f_{Z+2,N-2}^{(\pi)*})]_{\varepsilon\alpha}} \\ &\times \frac{(F_{Z,N}^{(\nu)*})_{\eta\delta}}{[(1 + F_{Z,N}^{(\nu)}(\theta) f_{Z+2,N-2}^{(\nu)*})]_{\gamma\eta}} \sin \theta d\theta. \end{aligned} \quad (26)$$

The required amplitudes ( $u_{im}$ ,  $v_{im}$ ) and expansion coefficients  $C_{ij,m}$  of axially symmetric HFB intrinsic state  $|\Phi_0\rangle$  with  $K = 0$  to evaluate the expressions  $n^J$ ,  $n_{(Z,N),(Z+2,N-2)}(\theta)$ ,  $f_{Z,N}$ , and

$F_{Z,N}(\theta)$  [50], are obtained by minimizing the expectation value of the effective Hamiltonian given by

$$H = H_{\text{sp}} + V(P) + V(QQ) + V(HH), \quad (27)$$

in a basis consisting of a set of deformed states. The details about the single particle Hamiltonian  $H_{\text{sp}}$  as well as the pairing  $V(P)$ , quadrupole-quadrupole  $V(QQ)$ , and hexadecapole-hexadecapole  $V(HH)$  parts of the effective two-body interaction have been given in Ref. [49]. To perform a statistical analysis, sets of 24 NTMEs  $M^{(0\nu)}$  for  $(\beta^-\beta^-)_{0\nu}$  decay are evaluated using Eq. (26) in conjunction with four different parametrizations of the two-body effective interaction, two sets of form factors, and three different parametrizations of the SRC. The details about the four different parametrizations have already been given in Refs. [49,50]. However, a brief discussion about them is presented here for the sake of completeness.

The strengths of the proton-proton, the neutron-neutron, and the proton-neutron parts of the  $V(QQ)$  are denoted by  $\chi_{2pp}$ ,  $\chi_{2nn}$ , and  $\chi_{2pn}$ , respectively. In Refs. [74,75], it has been shown that the experimental excitation energy of the  $2^+$  state,  $E_{2^+}$  can be fitted by taking equal strengths of the like particle components of the  $QQ$  interaction, i.e.,  $\chi_{2pp} = \chi_{2nn} = 0.0105$  MeV  $b^{-4}$  and by varying the strength of the proton-neutron component of the  $QQ$  interaction  $\chi_{2pn}$ . In Ref. [49], it was also feasible to employ an alternative isoscalar parametrization of the quadrupole-quadrupole interaction, by taking  $\chi_{2pp} = \chi_{2nn} = \chi_{2pn}/2$  and varying together the three

TABLE II. Calculated NTMEs  $M^{(0v)}$  in the PHFB model with four different parametrization of effective two-body interaction, namely (a)  $PQQ1$ , (b)  $PQQHH1$ , (c)  $PQQ2$ , and (d)  $PQQHH2$ , two different parametrizations of form factors and three different parametrizations of Jastrow type of SRC for the  $(\beta^- \beta^-)_{0v}$  decay of  $^{94,96}\text{Zr}$ ,  $^{98,100}\text{Mo}$ ,  $^{104}\text{Ru}$ ,  $^{110}\text{Pd}$ ,  $^{128,130}\text{Te}$ , and  $^{150}\text{Nd}$  isotopes due to the exchange of light Majorana neutrinos.

Nuclei	HOC1	HOC1 + SRC			HOC1 + SRC( $\bar{A}/2$ )			HOC2	HOC2 + SRC			
		SRC1	SRC2	SRC3	SRC1	SRC2	SRC3		SRC1	SRC2	SRC3	
$^{94}\text{Zr}$	(a)	4.3108	3.6776	4.2364	4.4187	4.0491	4.6377	4.8272	4.3293	3.6892	4.2533	4.4376
	(b)	3.9577	3.3702	3.8874	4.0567	3.7047	4.2496	4.4255	3.9747	3.3809	3.9030	4.0741
	(c)	4.1867	3.6645	4.1359	4.2867	4.0619	4.5584	4.7151	4.2020	3.6741	4.1499	4.3023
	(d)	3.7598	3.1949	3.6914	3.8541	3.5116	4.0347	4.2038	3.7762	3.2051	3.7064	3.8708
$^{96}\text{Zr}$	(a)	3.1099	2.6244	3.0489	3.1881	2.8994	3.3469	3.4916	3.1241	2.6332	3.0619	3.2026
	(b)	3.0805	2.5755	3.0155	3.1602	2.8321	3.2959	3.4464	3.0950	2.5845	3.0287	3.1751
	(c)	2.9718	2.5049	2.9128	3.0467	2.7665	3.1965	3.3357	2.9855	2.5134	2.9253	3.0606
	(d)	2.8923	2.4133	2.8301	2.9673	2.6533	3.0926	3.2353	2.9060	2.4219	2.8426	2.9813
$^{98}\text{Mo}$	(a)	7.0201	6.0809	6.9235	7.1942	6.7410	7.6293	7.9107	7.0483	6.0988	6.9495	7.2231
	(b)	6.5208	5.6151	6.4261	6.6871	6.1957	7.0506	7.3221	6.5477	5.6320	6.4507	6.7146
	(c)	7.0539	6.1054	6.9563	7.2296	6.7656	7.6626	7.9468	7.0824	6.1234	6.9826	7.2589
	(d)	6.4528	5.5523	6.3582	6.6178	6.1261	6.9758	7.2456	6.4796	5.5692	6.3828	6.6451
$^{100}\text{Mo}$	(a)	6.8305	5.8716	6.7394	7.0155	6.4712	7.3865	7.6736	6.8597	5.8902	6.7664	7.0454
	(b)	6.5255	5.5826	6.4329	6.7043	6.1305	7.0272	7.3096	6.5538	5.6005	6.4589	6.7333
	(c)	6.8843	5.9193	6.7925	7.0704	6.5244	7.4454	7.7344	6.9137	5.9379	6.8196	7.1005
	(d)	5.8838	5.0268	5.8000	6.0467	5.5173	6.3327	6.5892	5.9095	5.0431	5.8237	6.0730
$^{104}\text{Ru}$	(a)	4.9041	4.1810	4.8420	5.0500	4.6013	5.2990	5.5154	6.8597	5.8902	6.7664	7.0454
	(b)	4.5252	3.8308	4.4631	4.6627	4.1950	4.8624	5.0701	6.5538	5.6005	6.4589	6.7333
	(c)	4.6105	3.9296	4.5524	4.7483	4.3233	4.9807	5.1845	6.9137	5.9379	6.8196	7.1005
	(d)	4.1943	3.5472	4.1366	4.3227	3.8818	4.5039	4.6975	5.9095	5.0431	5.8237	6.0730
$^{110}\text{Pd}$	(a)	8.0959	6.9773	7.9906	8.3117	7.7645	8.8352	9.1697	8.1300	6.9989	8.0220	8.3467
	(b)	6.8084	5.8136	6.7118	6.9972	6.4371	7.3862	7.6834	6.8383	5.8326	6.7394	7.0279
	(c)	7.7679	6.6955	7.6660	7.9739	7.4533	8.4788	8.7995	7.8006	6.7163	7.6961	8.0074
	(d)	7.1998	6.1771	7.0999	7.3936	6.8577	7.8328	8.1386	7.2306	6.1966	7.1283	7.4252
$^{128}\text{Te}$	(a)	3.4090	2.9063	3.3533	3.4978	3.2453	3.7190	3.8698	3.4239	2.9157	3.3670	3.5130
	(b)	3.7254	3.1201	3.6599	3.8338	3.4477	4.0197	4.2012	3.7433	3.1313	3.6763	3.8520
	(c)	4.0718	3.4962	4.0110	4.1767	3.9073	4.4529	4.6257	4.0889	3.5070	4.0268	4.1942
	(d)	3.9541	3.3394	3.8875	4.0641	3.7048	4.2856	4.4700	3.9722	3.3507	3.9041	4.0827
$^{130}\text{Te}$	(a)	4.6291	4.0296	4.5729	4.7458	4.5157	5.0915	5.2720	4.6472	4.0410	4.5895	4.7643
	(b)	3.8628	3.2691	3.8033	3.9741	3.6204	4.1867	4.3651	3.8805	3.2802	3.8195	3.9922
	(c)	4.5565	3.9644	4.5007	4.6716	4.4422	5.0107	5.1890	4.5744	3.9756	4.5171	4.6898
	(d)	3.8553	3.2641	3.7959	3.9660	3.6160	4.1797	4.3573	3.8728	3.2751	3.8120	3.9840
$^{150}\text{Nd}$	(a)	3.3454	2.9312	3.3122	3.4317	3.3018	3.7068	3.8318	3.3583	2.9394	3.3241	3.4449
	(b)	2.5216	2.1896	2.4937	2.5894	2.4578	2.7810	2.8811	2.5319	2.1961	2.5032	2.5999
	(c)	3.2683	2.8630	3.2358	3.3528	3.2242	3.6206	3.7429	3.2809	2.8710	3.2475	3.3657
	(d)	2.6013	2.2655	2.5735	2.6703	2.5456	2.8730	2.9743	2.6117	2.2722	2.5832	2.6810

parameters to fit  $E_{2+}$ . These two alternative parametrizations of the quadrupole-quadrupole interaction were referred to as  $PQQ1$  and  $PQQ2$ . Two additional parametrizations, namely  $PQQHH1$  and  $PQQHH2$  were obtained with the inclusion of the hexadecapolar  $HH$  part of the effective interaction. Presently, we consider a form of Jastrow short-range correlations simulating the effects of Argonne V18, CD-Bonn potentials in the self-consistent CCM [62], given by

$$f(r) = 1 - ce^{-ar^2}(1 - br^2), \quad (28)$$

where  $a = 1.1 \text{ fm}^{-2}$ ,  $1.59 \text{ fm}^{-2}$ ,  $1.52 \text{ fm}^{-2}$ ,  $b = 0.68 \text{ fm}^{-2}$ ,  $1.45 \text{ fm}^{-2}$ ,  $1.88 \text{ fm}^{-2}$ , and  $c = 1.0$ ,  $0.92$ ,  $0.46$  for Miller and

Spencer parametrizations, Argonne  $NN$ , CD-Bonn potentials, which are denoted by SRC1, SRC2, and SRC3, respectively. Finally, the uncertainties associated with the NTMEs  $M^{(0v)}$  for  $(\beta^- \beta^-)_{0v}$  decay are evaluated by calculating the mean and standard deviation given by

$$\bar{M}^{(0v)} = \frac{\sum_{i=1}^N M_i^{(0v)}}{N}, \quad (29)$$

and

$$\Delta \bar{M}^{(0v)} = \frac{1}{\sqrt{N-1}} \left[ \sum_{i=1}^N (\bar{M}^{(0v)} - M_i^{(0v)})^2 \right]^{1/2}. \quad (30)$$

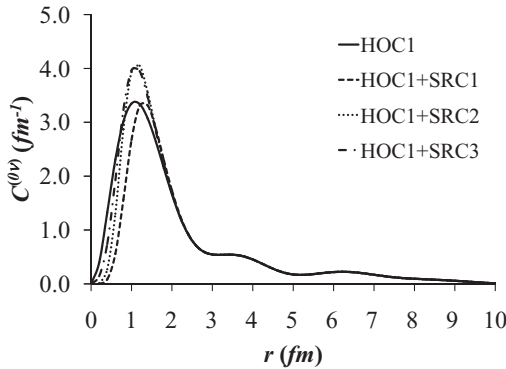


FIG. 2. Radial dependence of  $C^{(0v)}(r)$  for the  $(\beta^- \beta^-)_{0v}$  mode of  $^{100}\text{Mo}$  isotope.

### III. RESULTS AND DISCUSSIONS

In the present work, we use the same wave functions as used in the earlier works [50,51,74,75]. It has been already shown that [50] the experimental excitation energies of  $2^+$  state  $E_{2^+}$  [76] can be reproduced to about 98% accuracy by adjusting the proton-neutron quadrupolar correlation strength parameter  $\chi_{2pn}$  or  $\chi_{2pp}$ . The maximum change in  $E_{4^+}$  and  $E_{6^+}$  energies with respect to the  $PQQ1$  interaction [74,75] is about 8% and 31%, respectively. Further, the reduced  $B(E2:0^+ \rightarrow 2^+)$  transition probabilities, deformation parameters  $\beta_2$ , static quadrupole moments  $Q(2^+)$ , and gyromagnetic factors  $g(2^+)$  change by about 20%, 10% (except for the  $^{94}\text{Zr}$  and  $PQQ2$  interaction), 27% and 12% (except for the  $^{94,96}\text{Zr}$  and  $PQQ2$  interaction), respectively, and are usually in an overall agreement with the experimental data [77,78]. The experimental result for the quadrupole moment  $Q(2^+)$  of  $^{96}\text{Zr}$  is not available and the theoretical results exhibit a sign change for the  $PQQ2$  interaction. The theoretically calculated NTMEs  $M_{2v}$  for the  $0^+ \rightarrow 0^+$  transition also change up to approximately 11% except  $^{94}\text{Zr}$ ,  $^{128,130}\text{Te}$ , and  $^{150}\text{Nd}$  isotopes, for which the changes are approximately 42%, 21%, 24%, and 18%, respectively. The change in the ratio for deformation effect  $D_{2v}$  is approximately 18% but for  $^{94}\text{Zr}$  in which case the change is approximately 30%.

#### A. Exchange of light Majorana neutrinos

Employing the HFB wave functions generated with four different parametrizations of effective two-body interaction, the required NTMEs  $M^{(0v)}$  for  $^{94,96}\text{Zr}$ ,  $^{98,100}\text{Mo}$ ,  $^{104}\text{Ru}$ ,  $^{110}\text{Pd}$ ,  $^{128,130}\text{Te}$ , and  $^{150}\text{Nd}$  isotopes are calculated with the consideration of two sets of form factors and three different parametrizations of the Jastrow type of SRC. In Table I, the Fermi, Gamow-Teller, and tensor components of NTMEs  $M^{(0v)}$  for  $^{100}\text{Mo}$  are presented without (HOC—third column) and with the SRC (HOC + SRC—fourth to sixth columns) to exhibit the role of HOC as well as the SRC explicitly. To test the validity of closure approximation used in the present work, the NTMEs  $M^{(0v)}$  are also calculated for  $\bar{A}/2$  in the energy denominator in the case of HOC + SRC given in seventh to ninth columns of Table I. It is remarkable that the variation in the NTMEs calculated with FNS1 and FNS2 are almost negligible.

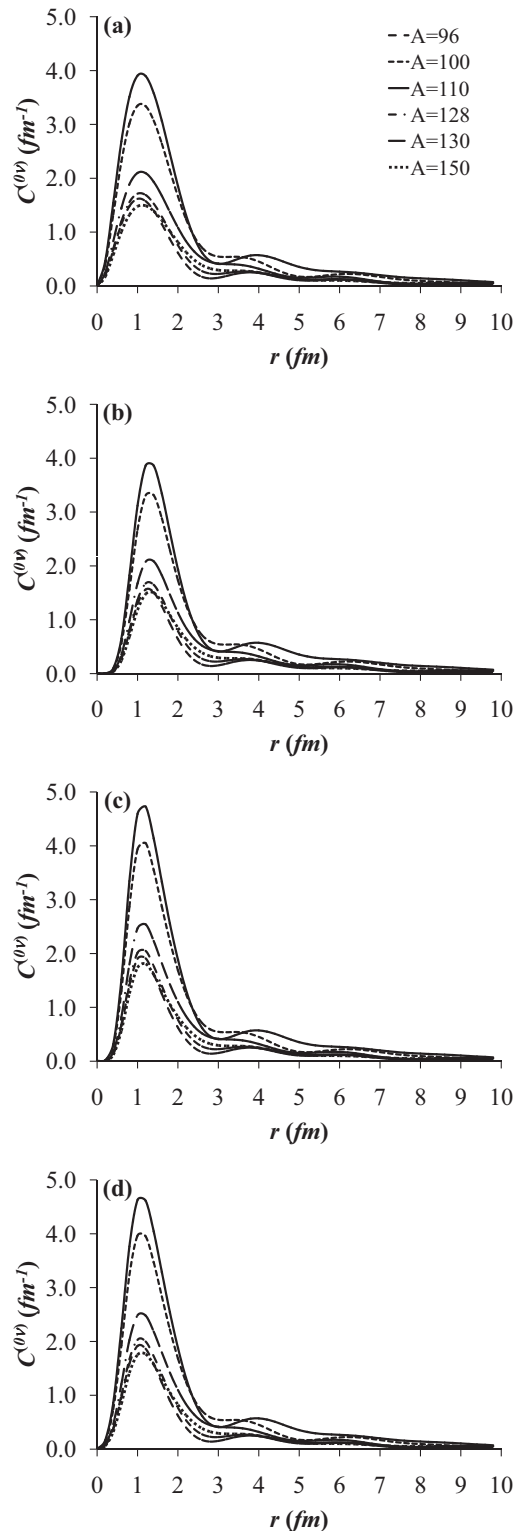


FIG. 3. Radial dependence of  $C^{(0v)}(r)$  for the  $(\beta^- \beta^-)_{0v}$  mode of  $^{96}\text{Zr}$ ,  $^{100}\text{Mo}$ ,  $^{110}\text{Pd}$ ,  $^{128,130}\text{Te}$ , and  $^{150}\text{Nd}$  isotopes. (a), (b), (c), and (d) correspond to HOC1, HOC1 + SRC1, HOC1 + SRC2, and HOC1 + SRC3, respectively.

In Table II, we present sets of 24 NTMEs  $M^{(0v)}$  for  $^{94,96}\text{Zr}$ ,  $^{98,100}\text{Mo}$ ,  $^{104}\text{Ru}$ ,  $^{110}\text{Pd}$ ,  $^{128,130}\text{Te}$ , and  $^{150}\text{Nd}$  isotopes calculated in the same approximations as mentioned above.

TABLE III. Changes (in %) of the NTMEs  $M^{(0v)}$  due to exchange of light Majorana neutrinos, for the  $(\beta^-\beta^-)_{0v}$  decay with the inclusion of FNS1, HOC1, and HOC1 + SRC (HOC1 + SRC1, HOC1 + SRC2, and HOC1 + SRC3) for the four different parametrizations of the effective two-body interaction, namely (a)  $PQQ1$ , (b)  $PQQHH1$ , (c)  $PQQ2$ , and (d)  $PQQHH2$ .

FNS1	HOC1	HOC1 + SRC
(a) 8.94–10.63	11.17–12.96	(i) 12.38–15.61 (ii) 0.99–1.96 (iii) 2.48–2.97
(b) 9.40–11.07	11.43–13.03	(i) 13.17–16.40 (ii) 1.11–2.11 (iii) 2.50–3.04
(c) 8.95–10.68	10.13–13.00	(i) 12.40–15.71 (ii) 0.99–1.99 (iii) 2.39–2.99
(d) 9.25–11.15	11.38–12.73	(i) 12.91–16.56 (ii) 1.07–2.15 (iii) 2.51–3.06

The sets of NTMEs calculated with FNS1 and FNS2 are denoted by HOC1 and HOC2, respectively. It is noticed in general but for  $^{128}\text{Te}$  isotope that the NTMEs evaluated for both  $PQQ1$  and  $PQQ2$  parametrizations are quite close. The inclusion of the hexadecapolar term tends to reduce them by magnitudes, specifically depending on the structure of nuclei. The maximum variation in  $M^{(0v)}$  due to the  $PQQHH1$ ,  $PQQ2$ , and  $PQQHH2$  parametrizations with respect to  $PQQ1$  one lies between 20–25%. The relative change in NTMEs  $M^{(0v)}$ , by changing the energy denominator to  $\bar{A}/2$  instead of  $\bar{A}$  is in between 8.7%–12.7%, which confirms that the dependence of NTMEs on average excitation energy  $\bar{A}$  is small and thus, the validity of the closure approximation for  $(\beta^-\beta^-)_{0v}$  decay is supported.

The study of the radial evolution of NTMEs defined by [71]

$$M^{(0v)} = \int C^{(0v)}(r) dr, \quad (31)$$

is the best possible tool to display the role of the HOC as well as the SRC. By the study of radial evolution of NTMEs  $M^{(0v)}$ , Šimkovic *et al.* in the QRPA [71] and Menéndez *et al.* in the ISM [79] have shown that the magnitude of  $M^{(0v)}$  for all nuclei undergoing  $(\beta^-\beta^-)_{0v}$  decay exhibit a maximum at about the internucleon distance  $r \approx 1$  fm, and that the contributions of decaying pairs coupled to  $J = 0$  and  $J > 0$  almost cancel out beyond  $r \approx 3$  fm. Similar observations on the radial evolution of NTMEs  $M^{(0v)}$  and  $M^{(0N)}$  due to the exchange of light [50] and heavy Majorana neutrinos [51], respectively, have also been reported within the PHFB approach.

In Fig. 2, the effects due to the HOC and SRC are made more transparent by plotting the radial dependence of  $C^{(0v)}$  for  $^{100}\text{Mo}$  isotope with the  $PQQ1$  parametrization of the effective two-body interaction in four cases, namely HOC1, HOC1 + SRC1, HOC1 + SRC2, and HOC1 + SRC3. In Fig. 3, the radial dependence of  $C^{(0v)}$  for the same four combinations of HOC1 and SRC are plotted for  $^{96}\text{Zr}$ ,  $^{100}\text{Mo}$ ,

TABLE IV. Deformation ratios  $D^{(0v)}$  of  $(\beta^-\beta^-)_{0v}$  decay for the  $PQQ1$  parametrization.

Nuclei	HOC1	HOC1 + SRC		
		SRC1	SRC2	SRC3
$^{94}\text{Zr}$	2.48	2.52	2.49	2.49
$^{96}\text{Zr}$	4.40	4.53	4.43	4.40
$^{98}\text{Mo}$	1.94	1.95	1.95	1.94
$^{100}\text{Mo}$	2.15	2.17	2.15	2.14
$^{104}\text{Ru}$	3.80	3.91	3.81	3.79
$^{110}\text{Pd}$	2.61	2.66	2.62	2.61
$^{128}\text{Te}$	4.38	4.50	4.40	4.38
$^{130}\text{Te}$	2.94	2.95	2.94	2.94
$^{150}\text{Nd}$	6.18	6.17	6.18	6.19

$^{110}\text{Pd}$ ,  $^{128,130}\text{Te}$ , and  $^{150}\text{Nd}$  isotopes. It is noticed that the  $C^{(0v)}$  are peaked at  $r = 1.0$  fm for the HOC1 and the addition of SRC1 and SRC2 shifts the peak to 1.25 fm. However, the position of the peak remains unchanged at  $r = 1.0$  fm with the inclusion of SRC3. Although, the radial distributions of  $C^{(0v)}$  extends up to about 10 fm, the maximum contribution to the radial evolution of  $M^{(0v)}$  results from the distribution of  $C^{(0v)}$  up to 3 fm. In addition, the above observations also remain valid with the other three parametrizations of the effective two-body interaction. The observed variation in the areas of curves in different cases is intimately related with the large changes in NTMEs  $M^{(0v)}$  presented in Table II.

In Table III, the relative changes in NTMEs  $M^{(0v)}$  (in %) due to the different approximations are presented. It is noticed that the consideration of FNS1 induces changes about 9.0%–11.0% in the NTMEs  $M_{VV}^{(0v)} + M_{AA}^{(0v)}$  of point nucleon case. The inclusion of HOC1 reduces the NTMEs further by 11.0%–13.0%. The NTMEs  $M^{(0v)}$  are approximately reduced by 13.0%–17.0%, 1.0%–2.0%, and 2.5%–3.0% with the addition of SRC1, SRC2, and SRC3, respectively, relative to the HOC1 case.

The effect of deformation on  $M^{(0v)}$  is quantified by the quantity  $D^{(0v)}$  defined as the ratio of  $M^{(0v)}$  at zero deformation ( $\zeta_{qq} = 0$ ) and full deformation ( $\zeta_{qq} = 1$ ) [80]:

$$D^{(0v)} = \frac{M^{(0v)}(\zeta_{qq} = 0)}{M^{(0v)}(\zeta_{qq} = 1)}. \quad (32)$$

In Table IV, we tabulate the values of  $D^{(0v)}$  for  $^{94,96}\text{Zr}$ ,  $^{98,100}\text{Mo}$ ,  $^{104}\text{Ru}$ ,  $^{110}\text{Pd}$ ,  $^{128,130}\text{Te}$ , and  $^{150}\text{Nd}$  nuclei. It is observed that owing to deformation effects, the NTMEs  $M^{(0v)}$  are suppressed by factor of about 2–6 in the mass range  $A = 90$ –150. Thus, the deformation plays a crucial role in the nuclear structure aspects of  $(\beta^-\beta^-)_{0v}$  decay.

In the present statistical analysis, we employ only the 24 NTMEs listed in the columns 4–6 (HOC1 + SRC) and columns 11–13 of Table II, employing the bare and quenched values of axial vector coupling constant  $g_A = 1.254$  and  $g_A = 1.0$ , respectively. In Table V, we display the calculated averages  $\overline{M}^{(0v)}$  and their variances  $\Delta\overline{M}^{(0v)}$  for  $^{94,96}\text{Zr}$ ,  $^{98,100}\text{Mo}$ ,  $^{110}\text{Pd}$ ,  $^{128,130}\text{Te}$ , and  $^{150}\text{Nd}$  isotopes along with all the available theoretical results in other models. It turns out that the uncertainties  $\Delta\overline{M}^{(0v)}$  are of the order of 10%, but for

TABLE V. Average NTMEs  $\overline{M}^{(0v)}$  and uncertainties  $\Delta\overline{M}^{(0v)}$  for the  $(\beta^-\beta^-)_{0v}$  decay of  $^{94}\text{Zr}$ ,  $^{98,100}\text{Mo}$ ,  $^{104}\text{Ru}$ ,  $^{110}\text{Pd}$ ,  $^{128,130}\text{Te}$ , and  $^{150}\text{Nd}$  isotopes. Both bare and quenched values of  $g_A$  are considered. Cases I and II denote calculations with and without SRC1, respectively. In the fifth column, (a)–(e) correspond to Jastrow, FHCh, UCOM, and CCM SRC with Argonne V18 and CD-Bonn potentials, respectively. The range of values in the QRPA and RQRPA for  $g_A = 1.0$  are tabulated.

Nuclei	$g_A$	Case I $\overline{M}^{(0v)}$	Case II $\overline{M}^{(0v)}$	SRC	QRPA [48]	RQRPA [48]	QRPA [60,81,82]	ISM [37,79]	EDF [57]	IBM [55]
$^{94}\text{Zr}$	1.254	$3.88 \pm 0.37$	$4.08 \pm 0.24$	(c)			$3.52 \pm 0.39$			
	1.0	$2.76 \pm 0.26$	$2.90 \pm 0.17$	(c)			$3.90 \pm 0.13$			
$^{96}\text{Zr}$	1.254	$2.86 \pm 0.26$	$3.03 \pm 0.12$	(a)	$1.22 \pm 0.03$	$1.31 \pm 0.15$				2.53
				(b)	$1.23 \pm 0.04$	$1.33 \pm 0.15$				
				(c)	$1.77 \pm 0.02$	$1.77 \pm 0.02$	3.117			5.65
				(d)	$2.07 \pm 0.10$	$2.01 \pm 0.17$				2.89
				(e)	$2.28 \pm 0.03$	$2.19 \pm 0.22$				3.00
	1.0	$2.04 \pm 0.19$	$2.16 \pm 0.09$		$1.32 \pm 0.08 -$	$1.22 \pm 0.12 -$				
					$2.11 \pm 0.12$	$1.88 \pm 0.16$	2.764			
$^{98}\text{Mo}$	1.254	$6.49 \pm 0.55$	$6.81 \pm 0.32$							
	1.0	$4.64 \pm 0.41$	$4.88 \pm 0.25$							
$^{100}\text{Mo}$	1.254	$6.26 \pm 0.63$	$6.59 \pm 0.44$	(a)	$3.64 \pm 0.21$	$3.03 \pm 0.21$				3.73
				(b)	$3.73 \pm 0.21$	$3.12 \pm 0.21$				
				(c)	$4.71 \pm 0.28$	$3.88 \pm 0.26$	3.931			5.08
				(d)	$5.18 \pm 0.36$	$4.20 \pm 0.24$				4.31
				(e)	$5.73 \pm 0.34$	$4.67 \pm 0.31$				4.50
	1.0	$4.49 \pm 0.47$	$4.73 \pm 0.33$		$2.96 \pm 0.15 -$	$2.55 \pm 0.13 -$	3.103			
					$4.44 \pm 0.24$	$3.75 \pm 0.21$				
$^{104}\text{Ru}$	1.254	$4.36 \pm 0.44$	$4.61 \pm 0.28$	(c)			$3.73 \pm 1.56$			
	1.0	$3.15 \pm 0.33$	$3.33 \pm 0.22$	(c)			$4.10 \pm 1.40$			
$^{110}\text{Pd}$	1.254	$7.16 \pm 0.74$	$7.53 \pm 0.54$	(a)						3.62
				(c)			$5.63 \pm 0.49$			
				(d)						4.15
				(e)						4.31
	1.0	$5.12 \pm 0.55$	$5.39 \pm 0.41$	(c)			$5.14 \pm 0.69$			
$^{128}\text{Te}$	1.254	$3.62 \pm 0.39$	$3.82 \pm 0.28$	(a)	$3.97 \pm 0.14$	$3.52 \pm 0.13$				4.48
				(b)	$4.15 \pm 0.15$	$3.68 \pm 0.14$				
				(c)	$5.04 \pm 0.15$	$4.45 \pm 0.15$	5.62			4.11
				(d)	$5.38 \pm 0.17$	$4.71 \pm 0.17$				4.97
				(e)	$5.99 \pm 0.17$	$5.26 \pm 0.16$				5.13
	1.0	$2.61 \pm 0.28$	$2.75 \pm 0.20$		$3.11 \pm 0.09 -$	$2.77 \pm 0.09 -$	3.74			
					$4.54 \pm 0.13$	$4.0 \pm 0.12$				
$^{130}\text{Te}$	1.254	$4.05 \pm 0.49$	$4.26 \pm 0.39$	(a)	$3.56 \pm 0.13$	$3.22 \pm 0.13$				4.03
				(b)	$3.72 \pm 0.14$	$3.36 \pm 0.15$				
				(c)	$4.53 \pm 0.12$	$4.07 \pm 0.13$	5.12			5.13
				(d)	$4.77 \pm 0.15$	$4.27 \pm 0.15$				4.47
				(e)	$5.37 \pm 0.13$	$4.80 \pm 0.14$				4.61
	1.0	$2.91 \pm 0.35$	$3.07 \pm 0.28$		$2.55 \pm 0.08 -$	$2.15 \pm 0.14 -$	3.48			
					$4.11 \pm 0.08$	$3.69 \pm 0.09$				
$^{150}\text{Nd}$	1.254	$2.83 \pm 0.42$	$2.96 \pm 0.39$	(a)	$2.95 \pm 0.04$					2.32
				(c)						1.71
				(d)						2.74
				(e)						2.88
	1.0	$2.04 \pm 0.31$	$2.13 \pm 0.29$							

$^{130}\text{Te}$  and  $^{150}\text{Nd}$  isotopes for which  $\Delta\overline{M}^{(0v)}$  are approximately 12% and 15%, respectively. Further, the effect due to the Miller-Spenser parametrization of Jastrow type of SRC is estimated by evaluating the same mean  $\overline{M}^{(0v)}$  and standard deviations  $\Delta\overline{M}^{(0v)}$  for 16 NTMEs calculated using SRC2 and SRC3 parametrizations. By excluding the NTMEs due

to SRC1 in the statistical analysis, the uncertainties reduce by 1.5%–5%.

The figure-of-merit defined by

$$C_{mm}^{(0v)} = \frac{10^{24} \times G_{01}}{m_e^2} |M^{(0v)}|^2, \quad (33)$$

TABLE VI. Average figure of merits  $\bar{C}_{mm}^{(0v)}$  and uncertainties  $\Delta\bar{C}_{mm}^{(0v)}$  for the  $(\beta^-\beta^-)_{0v}$  decay of  $^{94,96}\text{Zr}$ ,  $^{98,100}\text{Mo}$ ,  $^{104}\text{Ru}$ ,  $^{110}\text{Pd}$ ,  $^{128,130}\text{Te}$ , and  $^{150}\text{Nd}$  isotopes. Both bare and quenched values of  $g_A$  are considered. Case II denote calculations without SRC1.

Nuclei	$g_A$	Case II		Exp. $T_{1/2}^{(0v)}$ (yr)	Ref.	$\langle m_\nu \rangle$ (eV)	$T_{1/2}^{(0v)} (m_\nu = 0.05 \text{ eV})$	$\xi^{(0v)}$
		$\bar{C}_{mm}^{(0v)}$	$\Delta\bar{C}_{mm}^{(0v)}$					
$^{94}\text{Zr}$	1.254	0.1076	0.0125	$1.9 \times 10^{19}$	[85]	$6.99 \times 10^2$	$3.72_{-0.39}^{+0.49} \times 10^{27}$	16.74
	1.0	0.0545	0.0062			$9.83 \times 10^2$	$7.34_{-0.76}^{+0.95} \times 10^{27}$	11.91
$^{96}\text{Zr}$	1.254	2.0851	0.1592	$9.2 \times 10^{21}$	[21]	7.22	$1.92_{-0.14}^{+0.16} \times 10^{26}$	73.74
	1.0	1.0658	0.0856			10.10	$3.75_{-0.28}^{+0.33} \times 10^{26}$	52.72
$^{98}\text{Mo}$	1.254	0.0032	0.0003	$1.0 \times 10^{14}$	[86]	$1.78 \times 10^6$	$1.26_{-0.11}^{+0.13} \times 10^{29}$	2.87
	1.0	0.0016	0.0002			$2.48 \times 10^6$	$2.46_{-0.23}^{+0.28} \times 10^{29}$	2.06
$^{100}\text{Mo}$	1.254	7.7464	1.0044	$1.0 \times 10^{24}$	[87]	0.36	$5.16_{-0.59}^{+0.77} \times 10^{25}$	141.9
	1.0	3.9874	0.5466			0.50	$1.00_{-0.12}^{+0.16} \times 10^{26}$	101.8
$^{104}\text{Ru}$	1.254	0.2594	0.0318				$1.54_{-0.17}^{+0.22} \times 10^{27}$	25.98
	1.0	0.1354	0.0180				$2.96_{-0.35}^{+0.45} \times 10^{27}$	18.76
$^{110}\text{Pd}$	1.254	3.1058	0.4446	$6.0 \times 10^{17}$	[88]	$7.33 \times 10^2$	$1.29_{-0.16}^{+0.22} \times 10^{26}$	89.84
	1.0	1.5904	0.2398			$1.02 \times 10^3$	$2.52_{-0.33}^{+0.45} \times 10^{26}$	64.27
$^{128}\text{Te}$	1.254	0.1038	0.0148	$1.1 \times 10^{23}$	[89]	9.36	$3.86_{-0.48}^{+0.64} \times 10^{27}$	16.42
	1.0	0.0539	0.0076			12.98	$7.42_{-0.92}^{+1.22} \times 10^{27}$	11.84
$^{130}\text{Te}$	1.254	3.1488	0.5757	$3.0 \times 10^{24}$	[90]	0.32	$1.27_{-0.20}^{+0.28} \times 10^{26}$	90.32
	1.0	1.6295	0.2994			0.45	$2.46_{-0.38}^{+0.55} \times 10^{26}$	64.97
$^{150}\text{Nd}$	1.254	7.2330	1.8979	$1.8 \times 10^{22}$	[20]	2.77	$5.53_{-1.15}^{+1.97} \times 10^{25}$	136.3
	1.0	3.7480	0.9919			3.85	$1.07_{-0.22}^{+0.38} \times 10^{26}$	98.10

is another NTME related convenient quantity and is usually used in the analysis of experimental data. The arbitrary scaling factor  $10^{24}$  is used so that the  $C_{mm}^{(0v)}$  are of the order of unity. Recently, the phase space factors have been calculated by Kotila and Iachello [83] with screening correction. However, we evaluate the 24  $C_{mm}^{(0v)}$  using rescaled phase space factors of Boehm and Vogel [84] for  $g_A = 1.254$  and perform a statistical analysis for estimating the averages  $\bar{C}_{mm}^{(0v)}$  and uncertainties  $\Delta\bar{C}_{mm}^{(0v)}$ . In the third and fourth columns of Table VI, the averages  $\bar{C}_{mm}^{(0v)}$  and uncertainties  $\Delta\bar{C}_{mm}^{(0v)}$  are displayed. The uncertainties in  $\Delta\bar{C}_{mm}^{(0v)}$  are about twice of those of  $\Delta\bar{M}^{(0v)}$ .

The limits on the effective mass of light neutrino  $\langle m_\nu \rangle$  are extracted from the largest observed limits on half-lives  $T_{1/2}^{0v}$  of  $(\beta^-\beta^-)_{0v}$  decay using the average  $\bar{C}_{mm}^{(0v)}$ . It is observed that the extracted limits on  $\langle m_\nu \rangle$  for  $^{100}\text{Mo}$  and  $^{130}\text{Te}$  nuclei are 0.36 eV–0.50 eV and 0.32 eV–0.45 eV, respectively. In the last but one column of Table VI, the predicted half-lives of  $(\beta^-\beta^-)_{0v}$  decay of  $^{94,96}\text{Zr}$ ,  $^{98,100}\text{Mo}$ ,  $^{110}\text{Pd}$ ,  $^{128,130}\text{Te}$ , and  $^{150}\text{Nd}$  isotopes are given for  $\langle m_\nu \rangle = 50$  meV. In the last column of Table VI, we present the nuclear sensitivities, which are related to mass sensitivities, defined by [35]

$$\xi^{(0v)} = 10^8 \sqrt{G_{01}} |M^{(0v)}|, \quad (34)$$

with an arbitrary normalization factor  $10^8$  so that the nuclear sensitivities turn out to be order of unity. It is observed that

the nuclear sensitivities for  $(\beta^-\beta^-)_{0v}$  decay of  $^{100}\text{Mo}$ ,  $^{150}\text{Nd}$ ,  $^{130}\text{Te}$ ,  $^{110}\text{Pd}$ ,  $^{96}\text{Zr}$ ,  $^{104}\text{Ru}$ ,  $^{94}\text{Zr}$ ,  $^{128}\text{Te}$ , and  $^{98}\text{Mo}$  isotopes are in the decreasing order of their magnitudes.

## B. Majoron emission

In the classical Majoron model, the NTMEs  $M^{(0v\phi)}$  for the  $(\beta^-\beta^-\phi)_{0v}$  decay are same as the  $M^{(0v)}$  for  $(\beta^-\beta^-)_{0v}$  decay. Hence, the average NTMEs  $\bar{M}^{(0v\phi)}$  and uncertainties  $\Delta\bar{M}^{(0v\phi)}$  are the same as the  $\bar{M}^{(0v)}$  and  $\Delta\bar{M}^{(0v)}$ , respectively. The phase space factors  $G_{0M}$  for the  $0^+ \rightarrow 0^+$  transition of the  $(\beta^-\beta^-\phi)_{0v}$  decay mode have been calculated by Hirsch *et al.* [23] using  $g_A = 1.25$ . We calculate the phase space factors given in Table VII for the  $0^+ \rightarrow 0^+$  transition of  $^{94,96}\text{Zr}$ ,  $^{98,100}\text{Mo}$ ,  $^{104}\text{Ru}$  and  $^{110}\text{Pd}$ ,  $^{128,130}\text{Te}$ , and  $^{150}\text{Nd}$  isotopes with  $g_A = 1.254$ . The maximum difference between the two sets of phase space factors is less than 5%.

The extracted limits on the effective Majoron-neutrino coupling parameter  $\langle g_M \rangle$  form the largest limits on the observed half-lives  $T_{1/2}^{(0v\phi)}$  are given in Table VII. The most stringent extracted limit on  $\langle g_M \rangle < (2.22 - 3.09) \times 10^{-5}$ . In column 6 of the same Table VII, the predicted half-lives  $T_{1/2}^{(0v\phi)}$  for  $\langle g_M \rangle = 10^{-6}$  are displayed. The sensitivities  $\xi^{(0v\phi)}$  defined similar to  $\xi^{(0v)}$  are presented in the last column of Table VII. It is noticed that the sensitivities for the  $(\beta^-\beta^-\phi)_{0v}$  decay mode

TABLE VII. Phase space factors, extracted effective Majoron-neutrino coupling  $\langle g_M \rangle$ , predicted half-lives  $T_{1/2}^{(0\nu\phi)}$ , and sensitivities for the  $(\beta^- \beta^- \phi)_{0\nu}$  decay of  $^{94,96}\text{Zr}$ ,  $^{98,100}\text{Mo}$ ,  $^{104}\text{Ru}$ ,  $^{110}\text{Pd}$ ,  $^{128,130}\text{Te}$ , and  $^{150}\text{Nd}$  isotopes.

Nuclei	$G_{0M}$	Expt. $T_{1/2}^{(0\nu\phi)}$ (yr)	Ref.	$g_A$	$\langle g_M \rangle$	Predicted $T_{1/2}^{(0\nu\phi)}$ (yr) $\langle g_M \rangle = 10^{-6}$	$\xi^{(0\nu\phi)}$
$^{94}\text{Zr}$	$1.299 \times 10^{-17}$	$2.3 \times 10^{18}$	[85]	(a)	$4.49 \times 10^{-2}$	$4.63_{-0.50}^{+0.59} \times 10^{27}$	1.47
				(b)	$6.31 \times 10^{-2}$	$9.14_{-0.97}^{+1.15} \times 10^{27}$	1.05
$^{96}\text{Zr}$	$2.603 \times 10^{-15}$	$1.9 \times 10^{21}$	[21]	(a)	$1.49 \times 10^{-4}$	$4.19_{-0.30}^{+0.34} \times 10^{25}$	15.45
				(b)	$2.08 \times 10^{-4}$	$8.20_{-0.62}^{+0.70} \times 10^{25}$	11.04
$^{98}\text{Mo}$	$2.926 \times 10^{-21}$			(a)		$7.36_{-0.64}^{+0.74} \times 10^{30}$	0.04
				(b)		$1.44_{-0.14}^{+0.16} \times 10^{31}$	0.03
$^{100}\text{Mo}$	$1.736 \times 10^{-15}$	$2.7 \times 10^{22}$	[18]	(a)	$2.22 \times 10^{-5}$	$1.33_{-0.16}^{+0.20} \times 10^{25}$	27.45
				(b)	$3.09 \times 10^{-5}$	$2.58_{-0.33}^{+0.40} \times 10^{25}$	19.69
$^{104}\text{Ru}$	$3.037 \times 10^{-17}$			(a)		$1.55_{-0.18}^{+0.21} \times 10^{27}$	2.54
				(b)		$2.97_{-0.36}^{+0.44} \times 10^{27}$	1.83
$^{110}\text{Pd}$	$2.758 \times 10^{-16}$			(a)		$6.39_{-0.83}^{+1.03} \times 10^{25}$	12.51
				(b)		$1.25_{-0.17}^{+0.21} \times 10^{26}$	8.95
$^{128}\text{Te}$	$9.669 \times 10^{-18}$	$1.5 \times 10^{24}$	[91,92]	(a)	$6.88 \times 10^{-5}$	$7.09_{-0.93}^{+0.12} \times 10^{27}$	1.19
				(b)	$9.54 \times 10^{-5}$	$1.36_{-0.18}^{+0.22} \times 10^{28}$	0.86
$^{130}\text{Te}$	$1.300 \times 10^{-15}$			(a)		$4.23_{-0.68}^{+0.90} \times 10^{25}$	15.37
				(b)		$8.18_{-0.13}^{+0.18} \times 10^{25}$	11.05
$^{150}\text{Nd}$	$1.038 \times 10^{-14}$	$1.52 \times 10^{21}$	[20]	(a)	$8.50 \times 10^{-5}$	$1.10_{-0.24}^{+0.36} \times 10^{25}$	30.19
				(b)	$1.18 \times 10^{-4}$	$2.12_{-0.47}^{+0.71} \times 10^{25}$	21.73

of  $^{98}\text{Mo}$ ,  $^{128}\text{Te}$ ,  $^{94}\text{Zr}$ ,  $^{104}\text{Ru}$ ,  $^{110}\text{Pd}$ ,  $^{130}\text{Te}$ ,  $^{96}\text{Zr}$ ,  $^{100}\text{Mo}$ , and  $^{150}\text{Nd}$  isotopes are in the increasing order of their magnitudes.

### C. Sterile neutrinos

To estimate the uncertainties in NTMEs  $M^{(0\nu)}(m_h)$ , sets of 24 NTMEs are calculated for five potential  $(\beta^- \beta^- \phi)_{0\nu}$  candidates, namely  $^{96}\text{Zr}$ ,  $^{100}\text{Mo}$ ,  $^{128,130}\text{Te}$ , and  $^{150}\text{Nd}$  isotopes using HFB wave functions generated with four different parametrizations of effective two-body interaction, form factors with two different parametrizations, and three different

parametrizations of the Jastrow type of SRC in the mass range  $m_h = 10^{-4}$  MeV– $10^9$  MeV. It is noticed that in the limit  $m_h \rightarrow 0$ ,  $M^{(0\nu)}(m_h) \rightarrow M^{(0\nu)}$  and  $M^{(0\nu)}(m_h) \rightarrow (m_p m_e / m_h^2) M^{(0N)}$  in the limit  $m_h \rightarrow$  large. The extracted averages  $\bar{M}^{(0\nu)}(m_h)$  and uncertainties  $\Delta \bar{M}^{(0\nu)}(m_h)$  are presented in Table VIII. The uncertainties  $\Delta \bar{M}^{(0\nu)}(m_h)$  vary in between 4% (9%)–20% (36%) without (with) SRC1 depending on the considered mass of the sterile neutrinos. The extracted limits on the  $\nu_h - \nu_e$  mixing matrix element  $U_{eh}$  from the largest observed limits on the half-lives  $T_{1/2}^{0\nu}$  of  $(\beta^- \beta^-)_{0\nu}$  decay are displayed in

TABLE VIII. Calculated average NTMEs  $\bar{M}^{(0\nu)}(m_h)$  and uncertainties  $\Delta \bar{M}^{(0\nu)}(m_h)$  for the  $(\beta^- \beta^-)_{0\nu}$  decay of  $^{94,96}\text{Zr}$ ,  $^{98,100}\text{Mo}$ ,  $^{104}\text{Ru}$ ,  $^{110}\text{Pd}$ ,  $^{128,130}\text{Te}$ , and  $^{150}\text{Nd}$  isotopes. (a) Case I and (b) Case II denote calculations with and without SRC1, respectively.

Nuclei	$m_h = 10^{-4} - 1$ (MeV)	10	$10^2$	$10^3$	$10^4 - 10^9 \times 10^5 / m_h^2$
$^{96}\text{Zr}$	(a)	$2.863 \pm 0.260$	$2.692 \pm 0.252$	$1.273 \pm 0.170$	$0.050 \pm 0.015$
	(b)	$3.028 \pm 0.116$	$2.853 \pm 0.109$	$1.384 \pm 0.067$	$0.060 \pm 0.008$
$^{100}\text{Mo}$	(a)	$6.262 \pm 0.626$	$5.910 \pm 0.597$	$2.808 \pm 0.360$	$0.105 \pm 0.030$
	(b)	$6.589 \pm 0.438$	$6.229 \pm 0.405$	$3.028 \pm 0.188$	$0.124 \pm 0.016$
$^{128}\text{Te}$	(a)	$3.619 \pm 0.388$	$3.412 \pm 0.374$	$1.640 \pm 0.239$	$0.064 \pm 0.019$
	(b)	$3.819 \pm 0.278$	$3.607 \pm 0.263$	$1.776 \pm 0.153$	$0.076 \pm 0.011$
$^{130}\text{Te}$	(a)	$4.054 \pm 0.488$	$3.815 \pm 0.450$	$1.808 \pm 0.225$	$0.069 \pm 0.019$
	(b)	$4.262 \pm 0.392$	$4.018 \pm 0.349$	$1.949 \pm 0.104$	$0.081 \pm 0.010$
$^{150}\text{Nd}$	(a)	$2.831 \pm 0.422$	$2.659 \pm 0.396$	$1.213 \pm 0.198$	$0.043 \pm 0.013$
	(b)	$2.963 \pm 0.395$	$2.788 \pm 0.368$	$1.303 \pm 0.161$	$0.051 \pm 0.008$

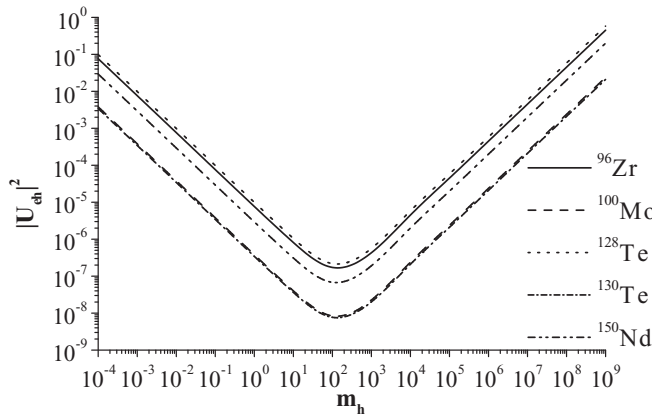


FIG. 4. Variation in extracted limits on the  $\nu_h - \nu_e$  mixing matrix element  $|U_{eh}|^2$  with the mass  $m_h$ .

Fig. 4. The extracted limits on the  $\nu_h - \nu_e$  mixing matrix element  $U_{eh}$  span a wider region of  $\nu_h$  mass  $m_h$  than those of laboratory experiments, astrophysical and cosmological observations [93], and are comparable to the limits obtained in Ref. [94].

#### IV. CONCLUSIONS

In the PHFB model, the NTMEs required to study the  $(\beta^- \beta^-)_{0\nu}$  decay of  $^{94,96}\text{Zr}$ ,  $^{98,100}\text{Mo}$ ,  $^{104}\text{Ru}$ ,  $^{110}\text{Pd}$ ,  $^{128,130}\text{Te}$ , and  $^{150}\text{Nd}$  isotopes within mechanisms involving the light Majorana neutrino, classical Majorons, and sterile neutrinos are calculated for four different parametrizations of pairing plus multipolar type of an effective two-body interaction, two sets of form factors, and three different parametrizations of SRC. It is observed that the closure approximation is quite valid as expected. The effect due to FNS is about 10% and the inclusion of the HOC further reduces the NTMEs by approximately 12%. With the consideration of the SRCs, the NTMEs are additionally reduced by 16.0% (1.0%) for SRC1 (SRC2). The effects due to deformation are between a factor of 2–6.

The sets of 24 NTMEs  $M^{(0\nu)}$  have been employed for estimating the uncertainties therein for the bare axial vector coupling constant  $g_A = 1.254$  and quenched value of  $g_A = 1.0$ . In the mechanisms involving light Majorana neutrino and classical Majorons, the uncertainties in NTMEs are in about 4.0% (9.0%)–13.5% (15.0%) without (with) the SRC1. In the case of sterile neutrinos, the uncertainties in NTMEs are in between 4% (9%)–20% (36%) depending on the considered mass of the sterile neutrinos without (with) SRC1.

We have also extracted limits on the effective neutrino mass  $\langle m_\nu \rangle$  from the available limits on experimental half-lives  $T_{1/2}^{0\nu}$  using average NTMEs  $\bar{M}^{(0\nu)}$  calculated in the PHFB model. In the case of the  $^{130}\text{Te}$  isotope, one obtains the best limit on the effective neutrino mass  $\langle m_\nu \rangle < 0.32 \text{ eV}-0.45 \text{ eV}$  from the observed limit on the half-life  $T_{1/2}^{0\nu} > 3.0 \times 10^{24} \text{ yr}$  of  $(\beta^- \beta^-)_{0\nu}$  decay [90]. The best limit on the Majoron-neutrino coupling constant  $\langle g_M \rangle$  turns out to be  $< 2.22 \times 10^{-5}$  from the observed half-life of the  $^{100}\text{Mo}$  isotope. The study of sensitivities of nuclei suggest that to extract the effective mass of light Majorana neutrino  $\langle m_\nu \rangle$ ,  $^{100}\text{Mo}$  is the preferred isotope and  $^{150}\text{Nd}$  is the favorable isotope to extract the  $\langle g_M \rangle$ . Thus, the sensitivities of different nuclei are mode dependent. It has been observed that the extracted limits on the sterile neutrino  $\nu_h - \nu_e$  mixing matrix element  $U_{eh}$  extend over a wider region of mass  $m_h$  than those of laboratory experiments, astrophysical and cosmological observations.

#### ACKNOWLEDGMENTS

This work is partially supported by the Council of Scientific and Industrial Research (CSIR), India vide sanction No. 03(1216)/12/EMR-II, Indo-Italian Collaboration DST-MAE project via grant no. INT/Italy/P-7/2012 (ER), Consejo Nacional de Ciencia y Tecnología (Conacyt)-México, and Dirección General de Asuntos del Personal Académico, Universidad Nacional Autónoma de México (DGAPA-UNAM) project no. IN103212. One of us (P.K.R.) thanks Prof. S. K. Singh, HNBG University, India for useful discussions.

- 
- [1] M. C. Gonzalez-Garcia and M. Maltoni, *Phys. Rep.* **460**, 1 (2008).
  - [2] S. M. Bilenky and C. Giunti, [arXiv:1203.5250v3](#) [hep-ph].
  - [3] H. V. Klapdor-Kleingrothaus, A. Dietz, H. L. Harney, and I. V. Krivosheina, *Mod. Phys. Lett. A* **16**, 2409 (2001); H. V. Klapdor-Kleingrothaus *et al.*, *Eur. Phys. J. A* **12**, 147 (2001).
  - [4] H. V. Klapdor-Kleingrothaus, I. V. Krivosheina, A. Dietz, and O. Chkvorets, *Phys. Lett. B* **586**, 198 (2004).
  - [5] F. Feruglio, A. Strumia, and F. Vissani, *Nucl. Phys. B* **637**, 345 (2002).
  - [6] C. E. Aalseth *et al.*, *Phys. Rev. D* **65**, 092007 (2002); *Mod. Phys. Lett. A* **17**, 1475 (2002).
  - [7] Yu. G. Zdesenko, F. A. Danevich, and V. I. Tretyak, *Phys. Lett. B* **546**, 206 (2002).
  - [8] A. Ianni, *Nucl. Instrum. Methods Phys. Res. A* **516**, 184 (2004).
  - [9] F. T. Avignone III, S. R. Elliott, and J. Engel, *Rev. Mod. Phys.* **80**, 481 (2008).
  - [10] J. D. Vergados, H. Ejiri, and F. Šimkovic, *Rep. Prog. Phys.* **75**, 106301 (2012).
  - [11] G. L. Fogli, E. Lisi, A. Marrone, A. Palazzo, and A. M. Rotunno, *Phys. Rev. D* **84**, 053007 (2011).
  - [12] H. V. Klapdor-Kleingrothaus, I. V. Krivosheina, and I. V. Titkova, *Int. J. Mod. Phys. A* **21**, 1159 (2006); H. V. Klapdor-Kleingrothaus and I. V. Krivosheina, *Mod. Phys. Lett. A* **21**, 1547 (2006).
  - [13] A. S. Barabash, *Phys. At. Nucl.* **73**, 162 (2010); *Phys. Part. Nucl.* **42**, 613 (2011).
  - [14] A. Giuliani, *Acta Phys. Pol. B* **41**, 1447 (2010).
  - [15] B. Schwingenheuer, [arXiv:1201.4916v1](#) [hep-ex].
  - [16] M. Doi and T. Kotani, *Prog. Theor. Phys.* **89**, 139 (1993).
  - [17] M. Hirsch, H. V. Klapdor-Kleingrothaus, and O. Panella, *Phys. Lett. B* **374**, 7 (1996).
  - [18] R. Arnold *et al.*, *Phys. Rev. Lett.* **107**, 062504 (2011); *Nucl. Phys. A* **765**, 483 (2006); **678**, 341 (2000).

- [19] A. Barabash and V. Brudanin (NEMO Collaboration), *Phys. At. Nucl.* **74**, 312 (2011).
- [20] J. Argyriades *et al.*, *Phys. Rev. C* **80**, 032501(R) (2009).
- [21] J. Argyriades *et al.*, *Nucl. Phys. A* **847**, 168 (2010).
- [22] P. Bamert, C. P. Burgess, and R. N. Mohapatra, *Nucl. Phys. B* **449**, 25 (1995).
- [23] M. Hirsch, H. V. Klapdor-Kleingrothaus, S. G. Kovalenko, and H. Päs, *Phys. Lett. B* **372**, 8 (1996).
- [24] A. Aguilar *et al.*, *Phys. Rev. D* **64**, 112007 (2001).
- [25] A. A. Aguilar-Arevalo *et al.*, *Phys. Rev. Lett.* **105**, 181801 (2010).
- [26] G. Mention, M. Fechner, T. Lasserre, T. A. Mueller, D. Lhuillier, M. Cribier, and A. Letourneau, *Phys. Rev. D* **83**, 073006 (2011).
- [27] Th. A. Mueller *et al.*, *Phys. Rev. C* **83**, 054615 (2011).
- [28] P. Huber, *Phys. Rev. C* **84**, 024617 (2011).
- [29] C. Giunti and M. Laveder, *Nucl. Phys. B Proc. Suppl.* **217**, 193 (2011).
- [30] A. Pilaftsis, *Phys. Rev. D* **49**, 2398 (1994).
- [31] P. Beneš, A. Faessler, S. Kovalenko, and F. Šimkovic, *Phys. Rev. D* **71**, 077901 (2005).
- [32] W. C. Haxton and G. J. Stephenson, Jr., *Prog. Part. Nucl. Phys.* **12**, 409 (1984).
- [33] M. Doi, T. Kotani, and E. Takasugi, *Prog. Theor. Phys. Suppl.* **83**, 1 (1985).
- [34] T. Tomoda, *Rep. Prog. Phys.* **54**, 53 (1991).
- [35] F. Šimkovic, G. Pantelis, J. D. Vergados, and A. Faessler, *Phys. Rev. C* **60**, 055502 (1999).
- [36] J. D. Vergados, *Phys. Rep.* **361**, 1 (2002).
- [37] E. Caurier, J. Menéndez, F. Nowacki, and A. Poves, *Phys. Rev. Lett.* **100**, 052503 (2008).
- [38] J. Barea and F. Iachello, *Phys. Rev. C* **79**, 044301 (2009).
- [39] E. Caurier, A. Poves, and A. P. Zuker, *Phys. Lett. B* **252**, 13 (1990); E. Caurier, F. Nowacki, A. Poves, and J. Retamosa, *Phys. Rev. Lett.* **77**, 1954 (1996); *Nucl. Phys. A* **654**, 973c (1999); E. Caurier, F. Nowacki, and A. Poves, *Eur. Phys. J. A* **36**, 195 (2008).
- [40] M. Horoi and S. Stoica, *Phys. Rev. C* **81**, 024321 (2010).
- [41] M. Horoi and B. A. Brown, [arXiv:1301.0256v1 \[nucl-th\]](#).
- [42] P. Vogel and M. R. Zirnbauer, *Phys. Rev. Lett.* **57**, 3148 (1986).
- [43] O. Civitarese, A. Faessler, and T. Tomoda, *Phys. Lett. B* **194**, 11 (1987).
- [44] J. Suhonen and O. Civitarese, *Phys. Rep.* **300**, 123 (1998).
- [45] A. Faessler and F. Šimkovic, *J. Phys. G* **24**, 2139 (1998).
- [46] F. Šimkovic, L. Pacearescu, and A. Faessler, *Nucl. Phys. A* **733**, 321 (2004); L. Pacearescu, A. Faessler, and F. Šimkovic, *Phys. At. Nucl.* **67**, 1210 (2004); R. Alvarez-Rodriguez, P. Sarriuguren, E. Moya de Guerra, L. Pacearescu, A. Faessler, and F. Šimkovic, *Phys. Rev. C* **70**, 064309 (2004); M. S. Yousef, V. Rodin, A. Faessler, and F. Šimkovic, *ibid.* **79**, 014314 (2009).
- [47] D. L. Fang, A. Faessler, V. Rodin, and F. Šimkovic, *Phys. Rev. C* **83**, 034320 (2011); **82**, 051301(R) (2010).
- [48] A. Faessler, V. Rodin, and F. Šimkovic, *J. Phys. G: Nucl. Part. Phys.* **39**, 124006 (2012).
- [49] R. Chandra, K. Chaturvedi, P. K. Rath, P. K. Raina, and J. G. Hirsch, *Europhys. Lett.* **86**, 32001 (2009).
- [50] P. K. Rath, R. Chandra, K. Chaturvedi, P. K. Raina, and J. G. Hirsch, *Phys. Rev. C* **82**, 064310 (2010).
- [51] P. K. Rath, R. Chandra, P. K. Raina, K. Chaturvedi, and J. G. Hirsch, *Phys. Rev. C* **85**, 014308 (2012).
- [52] P. K. Rath, R. Chandra, K. Chaturvedi, P. Lohani, P. K. Raina, and J. G. Hirsch, *Phys. Rev. C* **87**, 014301 (2013).
- [53] J. G. Hirsch, O. Castaños, and P. O. Hess, *Nucl. Phys. A* **582**, 124 (1995).
- [54] F. Iachello, J. Barea, and J. Kotila, *AIP Conf. Proc.* **1417**, 62 (2011); F. Iachello and J. Barea, *Nucl. Phys. B Proc. Suppl.* **217**, 5 (2011).
- [55] J. Barea, J. Kotila, and F. Iachello, *Phys. Rev. C* **87**, 014315 (2013).
- [56] N. Yosida and F. Iachello, [arXiv:1301.7172v1 \[nucl-th\]](#).
- [57] T. R. Rodríguez and G. Martínez-Pinedo, *Phys. Rev. Lett.* **105**, 252503 (2010).
- [58] G. A. Miller and J. E. Spencer, *Ann. Phys. (NY)* **100**, 562 (1976).
- [59] H. F. Wu, H. Q. Song, T. T. S. Kuo, W. K. Cheng, and D. Strottman, *Phys. Lett. B* **162**, 227 (1985).
- [60] M. Kortelainen and J. Suhonen, *Phys. Rev. C* **76**, 024315 (2007).
- [61] M. Kortelainen, O. Civitarese, J. Suhonen, and J. Toivanen, *Phys. Lett. B* **647**, 128 (2007).
- [62] F. Šimkovic, A. Faessler, H. Müther, V. Rodin, and M. Stauff, *Phys. Rev. C* **79**, 055501 (2009).
- [63] J. Menéndez, D. Gazit, and A. Schwenk, *Phys. Rev. Lett.* **107**, 062501 (2011).
- [64] P. Vogel, in *Current Aspects of Neutrino Physics*, edited by D. O. Caldwell (Springer, Berlin, 2001), Chap. 8, p. 177; [arXiv:nucl-th/0005020](#).
- [65] John N. Bahcall, Hitoshi Murayama, and C. Peña-Garay, *Phys. Rev. D* **70**, 033012 (2004).
- [66] F. T. Avignone III, G. S. King III, and Yu. G. Zdesenko, *New J. Phys.* **7**, 6 (2005); F. T. Avignone III, *Prog. Part. Nucl. Phys.* **57**, 170 (2006).
- [67] S. M. Bilenky and J. A. Grifols, *Phys. Lett. B* **550**, 154 (2002).
- [68] V. A. Rodin, A. Faessler, F. Šimkovic, and P. Vogel, *Phys. Rev. C* **68**, 044302 (2003).
- [69] J. Suhonen, *Phys. Lett. B* **607**, 87 (2005).
- [70] V. A. Rodin, A. Faessler, F. Šimkovic, and P. Vogel, *Nucl. Phys. A* **766**, 107 (2006); **793**, 213 (2007).
- [71] F. Šimkovic, A. Faessler, V. Rodin, P. Vogel, and J. Engel, *Phys. Rev. C* **77**, 045503 (2008).
- [72] P. Stoler, *Phys. Rep.* **226**, 103 (1993).
- [73] M. Doi, T. Kotani, and E. Takasugi, *Phys. Rev. D* **37**, 2575 (1988).
- [74] R. Chandra, J. Singh, P. K. Rath, P. K. Raina, and J. G. Hirsch, *Eur. Phys. J. A* **23**, 223 (2005).
- [75] S. Singh, R. Chandra, P. K. Rath, P. K. Raina, and J. G. Hirsch, *Eur. Phys. J. A* **33**, 375 (2007).
- [76] M. Sakai, *At. Data Nucl. Data Tables* **31**, 399 (1984).
- [77] S. Raman, C. W. Nestor, Jr., and P. Tikkanen, *At. Data Nucl. Data Tables* **78**, 1 (2001).
- [78] P. Raghavan, *At. Data Nucl. Data Tables* **42**, 189 (1989).
- [79] J. Menéndez, A. Poves, E. Caurier, and F. Nowacki, *Nucl. Phys. A* **818**, 139 (2009).
- [80] K. Chaturvedi, R. Chandra, P. K. Rath, P. K. Raina, and J. G. Hirsch, *Phys. Rev. C* **78**, 054302 (2008).
- [81] J. Suhonen and O. Civitarese, *Nucl. Phys. A* **847**, 207 (2010).
- [82] J. Suhonen, *Nucl. Phys. A* **853**, 36 (2010).
- [83] J. Kotila and F. Iachello, *Phys. Rev. C* **85**, 034316 (2012).
- [84] F. Boehm and P. Vogel, *Physics of Massive Neutrinos*, 2nd ed. (Cambridge University Press, Cambridge, 1992), p. 163.
- [85] R. Arnold *et al.*, *Nucl. Phys. A* **658**, 299 (1999).

- [86] J. H. Fremlin and M. C. Walters, *Proc. Phys. Soc. Lond. A* **65**, 911 (1952).
- [87] V. I. Tretyak (NEMO-3 Collaboration), *AIP Conf. Proc.* **1417**, 125 (2011).
- [88] R. G. Winter, *Phys. Rev.* **85**, 687 (1952).
- [89] C. Arnaboldi *et al.*, *Phys. Lett. B* **557**, 167 (2003).
- [90] C. Arnaboldi *et al.*, *Phys. Rev. C* **78**, 035502 (2008).
- [91] O. K. Manuel, *J. Phys. G* **17**, 221 (1991).
- [92] A. S. Barabash, *Phys. Rev. C* **81**, 035501 (2010).
- [93] A. D. Dolgov, S. H. Hansen, G. Raffelt, and D. V. Semikoz, *Nucl. Phys. B* **590**, 562 (2000); **580**, 331 (2000).
- [94] M. Blennow, E. Fernandez-Martinez, J. Lopez-Pavon, and J. Menéndez, *JHEP* **07** (2010) 096.